J|A|C|S
ARTICLES

Published on Web 05/13/2010

Structural Properties and Dynamic Behavior of Nonfibrillar Oligomers Formed by PrP(106−126)

Patrick Walsh,[†,‡] Philipp Neudecker,[‡,§,⊥] and Simon Sharpe*[,†,‡]

Molecular Structure and Function Programme, The Hospital for Sick Children, 555 University Avenue, Toronto, Ontario M5G 1X8, Canada, and Department of Biochemistry, Department of Molecular Genetics, and Department of Chemistry, University of Toronto, 1 King's College Circle, Toronto, Ontario M5S 1A8, Canada

Received January 17, 2010; E-mail: ssharpe@sickkids.ca

Abstract: The formation of nonfibrillar oligomers has been proposed as a common element of the aggregation pathway of proteins and peptides associated with neurodegenerative diseases such as Alzheimer's and Creutzfeldt−Jakob disease. While fibrillar structures have long been considered indicators of diseases linked with the accumulation of amyloid plaques, it has more recently been proposed that amyloid oligomers are in fact the cytotoxic form. Here we describe the local structure and dynamics of stable oligomers formed by a peptide comprising residues 106−126 of the human prion protein (PrP). Structural constraints from solid-state NMR reveal quaternary packing interactions within the hydrophobic core, similar to those previously reported for amyloid fibrils formed by this peptide, and consistent with structural studies of oligomers formed by the Alzheimer's β-amyloid peptide. However, a hydration-dependent increase in disorder is observed for nonfibrillar oligomers of PrP(106−126). In solution NMR spectra we observe narrow ^{1}H and ^{13}C resonances corresponding to a monomer in exchange with the ∼30 nm diameter nonfibrillar oligomers, giving additional information on the molecular structure of these species. Taken together, our data support a model in which the local structure of the oligomers contains the basic elements of amyloid fibrils, but with long-range disorder and local mobility that distinguishes these assemblies from the fibrillar form of PrP(106−126). These characteristics may provide a basis for the differing biological activities of amyloid fibrils and oligomers.

Introduction

Neurodegeneration associated with protein misfolding is characteristic of several human diseases including Alzheimer's, Parkinson's, and prion diseases. In each case, one of the primary pathological markers is the presence of proteinaceous plaques containing amyloid fibrils formed by the misfolded protein. Despite initial suggestions that formation of fibrils directly results in cytotoxicity, it is currently hypothesized that nonfibrillar oligomers are responsible for neuronal cell death and disease progression.[1−3] Nonfibrillar oligomers have been observed for a number of amyloid proteins and peptides *in vivo* and *in vitro*, including the Alzheimer's β-amyloid protein (Aβ), α-synuclein, and IAPP.[4−7] The discovery of antibodies that recognize oligomers formed by several amyloid peptides suggests that these assemblies share common structural elements.[1] In addition, nonfibrillar oligomers exhibit a marked increase in toxicity relative to their fibrillar counterparts, which is largely attributed to their membrane-disrupting ability, and which has been proposed to represent a common mechanism for the degenerative nature of amyloid diseases.[8−10]

Recent studies on amyloid forming peptides and proteins have shed light on the structural properties of amyloid fibrils.[11−15] The cross-β motif, in which the protein forms β-strands perpendicular to the long axis of the fibril, has been observed in several fibril structures, including Aβ_{1-40},[12] amylin,[14,16] and crystals of several short amyloid peptides.[13] In each case, the core of the protein contains a dehydrated interface between

[†] Molecular Structure and Function Programme, The Hospital for Sick Children.
[‡] Department of Biochemistry, University of Toronto.
[§] Department of Molecular Genetics, University of Toronto.
[⊥] Department of Chemistry, University of Toronto.

(1) Kayed, R.; Head, E.; Thompson, J. L.; McIntire, T. M.; Milton, S. C.; Cotman, C. W.; Glabe, C. G. *Science* **2003**, *300*, 486–489.
(2) Bucciantini, M.; Giannoni, E.; Chiti, F.; Baroni, F.; Formigli, L.; Zurdo, J.; Taddei, N.; Ramponi, G.; Dobson, C. M.; Stefani, M. *Nature* **2002**, *416*, 507–511.
(3) Caughey, B.; Lansbury, P. T. *Annu. Rev. Neurosci.* **2003**, *26*, 267–298.
(4) Conway, K. A.; Lee, S. J.; Rochet, J. C.; Ding, T. T.; Williamson, R. E.; Lansbury, P. T., Jr. *Proc. Natl. Acad. Sci. U.S.A.* **2000**, *97*, 571–576.
(5) Kayed, R.; Bernhagen, J.; Greenfield, N.; Sweimeh, K.; Brunner, H.; Voelter, W.; Kapurniotu, A. *J. Mol. Biol.* **1999**, *287*, 781–796.
(6) Walsh, D. M.; Klyubin, I.; Fadeeva, J. V.; Cullen, W. K.; Anwyl, R.; Wolfe, M. S.; Rowan, M. J.; Selkoe, D. J. *Nature* **2002**, *416*, 535–539.
(7) Haass, C.; Selkoe, D. J. *Nat. Rev. Mol. Cell Biol.* **2007**, *8*, 101–112.
(8) Kayed, R.; Sokolov, Y.; Edmonds, B.; McIntire, T. M.; Milton, S. C.; Hall, J. E.; Glabe, C. G. *J. Biol. Chem.* **2004**, *279*, 46363–46366.
(9) Glabe, C. G. *J. Biol. Chem.* **2008**, *283*, 29639–29643.
(10) Sokolov, Y.; Kozak, J. A.; Kayed, R.; Chanturiya, A.; Glabe, C. G.; Hall, J. E. *J. Gen. Physiol.* **2006**, *128*, 637–647.
(11) Jaroniec, C. P.; MacPhee, C. E.; Bajaj, V. S.; McMahon, M. T.; Dobson, C. M.; Griffin, R. G. *Proc. Natl. Acad. Sci. U.S.A.* **2004**, *101*, 711–716.
(12) Petkova, A. T.; Ishii, Y.; Balbach, J. J.; Antzutkin, O. N.; Leapman, R. D.; Delaglio, F.; Tycko, R. *Proc. Natl. Acad. Sci. U.S.A.* **2002**, *99*, 16742–16747.

 10.1021/ja100431q

stacked β-sheets, creating a 'steric-zipper', as described by Sawaya et al.[13] Illustrating the potential for variations on this theme, a recently reported structure for the Het-S yeast prion revealed β-solenoid or β-helical packing rather than a steric zipper in the core of the protein.[17] A similar arrangement has been proposed for the amyloid-like filaments formed by the *Escherichia coli* curli protein.[18]

In contrast to amyloid fibrils, relatively little is known regarding the molecular structure of nonfibrillar amyloid oligomers. A detailed characterization is of considerable interest since oligomers formed by several amyloid proteins have been shown to cause cell death in cultured neurons[19] as well as endothelial cells.[20,21] The observation that these species cause disruption of calcium regulation, in combination with several experiments suggesting that amyloid peptides can form conductive channels in planar bilayers,[22−24] has led to the concept that channel formation is an important aspect of oligomer cytotoxicity.[8,22,25] Other possible mechanisms which have been proposed include a nonspecific disruption of membranes, possibly through insertion of hydrophobic segments into the plasma membrane or through surface-mediated nucleation of fibril formation.[26−28] The induction of apoptosis in cultured neurons by amyloid oligomers has been reported, although a mechanism for this has not been revealed.[29,30]

High-resolution structural studies of nonfibrillar amyloid oligomers have been limited to Aβ_{1-40} and Aβ_{1-42} and have provided strong evidence that these species are composed of β-sheets with significant intermolecular strand formation.[31,32] Solid-state NMR studies reported by Chimon et al. revealed fibril-like packing within the β-sheet containing cores of large Aβ_{1-40} oligomers.[31] A significantly different organization of inter- and intramolecular β-sheets was observed for small 16−64 kDa detergent-stabilized globulomers of Aβ_{1-42}.[32] In contrast, NMR data reported for pore-forming oligomers of α-synuclein suggest a poorly ordered assembly with secondary structure distinct from α-synuclein fibrils.[33] Thus, questions remain regarding the potential for common elements that result in the cytotoxicity of nonfibrillar amyloid oligomers.

As a model for investigating the structures accessible to amyloid peptides we have focused on a 21-residue peptide derived from the mammalian prion protein (PrP). This peptide, PrP(106−126), forms amyloid fibrils[34−36] as well as cytotoxic nonfibrillar oligomers,[1,8] the latter of which have been proposed to either form ion channels[22,23,37] or induce a disruption of cellular membranes.[38] Previously, we have used solid-state NMR to determine the structure of amyloid fibrils formed by PrP(106−126), revealing a class 1 steric zipper motif.[15] Additionally, we have reported an initial biophysical characterization of membrane-disrupting, nonfibrillar oligomers of PrP(106−126), in which dynamic light scattering (DLS), transmission electron microscopy (TEM), and solid-state NMR were used to define the morphology and secondary structure of these species. They were observed to be large, roughly spherical structures with largely β-sheet secondary structure and a hydrodynamic radius of approximately 30 nm.[39]

Here, we present a comprehensive NMR investigation of the local structure and dynamics of PrP(106−126) in nonfibrillar oligomers. We find that these assemblies contain subunits with secondary and quaternary structure with strong similarity to those of the fibrillar form of this peptide. In particular, dipolar recoupling experiments indicate the presence of a parallel, in-register β-sheet structure, with sheets stacked in an antiparallel fashion to form fibril-like subunits. Solution NMR reveals the presence of a small population of structured monomers in rapid equilibrium with the large oligomers. Additional data suggest increased local motions and potential long-range disorder in the nonfibrillar oligomers relative to amyloid fibrils. On the basis of these data, a putative model for the oligomeric assembly of PrP(106−126) is presented.

Experimental Section

PrP(106−126) Preparations. PrP(106−126) was obtained from the Advanced Protein Technology Centre at the Hospital for Sick children with ^{13}C and ^{15}N amino acids obtained from Cambridge Isotope Laboratories. Peptides were prepared by solid-phase peptide synthesis, using standard FMOC chemistry. Six labeling schemes were devised, with incorporation of ^{13}C- and ^{15}N-labeled amino acids at selected sites as previously described[15] (Supporting Information, Table S1). The final product was purified in each case by reverse-phase HPLC, using an 11 mm × 300 mm C8 peptide

(13) Sawaya, M. R.; Sambashivan, S.; Nelson, R.; Ivanova, M. I.; Sievers, S. A.; Apostol, M. I.; Thompson, M. J.; Balbirnie, M.; Wiltzius, J. J.; McFarlane, H. T.; Madsen, A. O.; Riekel, C.; Eisenberg, D. *Nature* **2007**, *447*, 453–457.
(14) Luca, S.; Yau, W. M.; Leapman, R.; Tycko, R. *Biochemistry* **2007**, *46*, 13505–13522.
(15) Walsh, P.; Simonetti, K.; Sharpe, S. *Structure* **2009**, *17*, 417–426.
(16) Wiltzius, J. J.; Sievers, S. A.; Sawaya, M. R.; Cascio, D.; Popov, D.; Riekel, C.; Eisenberg, D. *Protein Sci.* **2008**, *17*, 1467–1474.
(17) Wasmer, C.; Lange, A.; Van Melckebeke, H.; Siemer, A. B.; Riek, R.; Meier, B. H. *Science* **2008**, *319*, 1523–6.
(18) Shewmaker, F.; McGlinchey, R. P.; Thurber, K. R.; McPhie, P.; Dyda, F.; Tycko, R.; Wickner, R. B. *J. Biol. Chem.* **2009**, *1*, 1.
(19) Lambert, M. P.; Barlow, A. K.; Chromy, B. A.; Edwards, C.; Freed, R.; Liosatos, M.; Morgan, T. E.; Rozovsky, I.; Trommer, B.; Viola, K. L.; Wals, P.; Zhang, C.; Finch, C. E.; Krafft, G. A.; Klein, W. L. *Proc. Natl. Acad. Sci. U.S.A.* **1998**, *95*, 6448–6453.
(20) Bhatia, R.; Lin, H.; Lal, R. *FASEB J.* **2000**, *14*, 1233–1243.
(21) Zhu, Y. J.; Lin, H.; Lal, R. *FASEB J.* **2000**, *14*, 1244–1254.
(22) Lin, M. C.; Mirzabekov, T.; Kagan, B. L. *J. Biol. Chem.* **1997**, *272*, 44–47.
(23) Kourie, J. I.; Culverson, A. L. *J. Neurosci. Res.* **2000**, *62*, 120–133.
(24) Kourie, J. I.; Farrelly, P. V.; Henry, C. L. *J. Neurosci. Res.* **2001**, *66*, 214–220.
(25) Pollard, H. B.; Arispe, N.; Rojas, E. *Cell. Mol. Neurobiol.* **1995**, *15*, 513–526.
(26) Yip, C. M.; Darabie, A. A.; McLaurin, J. *J. Mol. Biol.* **2002**, *318*, 97–107.
(27) McLaurin, J.; Chakrabartty, A. *J. Biol. Chem.* **1996**, *271*, 26482–26489.
(28) McLaurin, J.; Chakrabartty, A. *Eur. J. Biochem.* **1997**, *245*, 355–363.
(29) O'Donovan, C. N.; Tobin, D.; Cotter, T. G. *J. Biol. Chem.* **2001**, *276*, 43516–43523.
(30) Carimalo, J.; Cronier, S.; Petit, G.; Peyrin, J. M.; Boukhtouche, F.; Arbez, N.; Lemaigre-Dubreuil, Y.; Brugg, B.; Miquel, M. C. *Eur. J. Neurosci.* **2005**, *21*, 2311–2319.
(31) Chimon, S.; Shaibat, M. A.; Jones, C. R.; Calero, D. C.; Aizezi, B.; Ishii, Y. *Nat. Struct. Mol. Biol.* **2007**, *14*, 1157–1164.
(32) Yu, L.; et al. *Biochemistry* **2009**, *48*, 1870−1877.
(33) Kim, H.-Y.; Cho, M.-K.; Kumar, A.; Maier, E.; Siebenhaar, C.; Becker, S.; Fernandez, C. O.; Lashuel, H. A.; Benz, R.; Lange, A.; Zweckstetter, M. *J. Am. Chem. Soc.* **2009**, *131*, 17482–17489.
(34) Forloni, G.; Angeretti, N.; Chiesa, R.; Monzani, E.; Salmona, M.; Bugiani, O.; Tagliavini, F. *Nature* **1993**, *362*, 543–546.
(35) Selvaggini, C.; De Gioia, L.; Cantu, L.; Ghibaudi, E.; Diomede, L.; Passerini, F.; Forloni, G.; Bugiani, O.; Tagliavini, F.; Salmona, M. *Biochem. Biophys. Res. Commun.* **1993**, *194*, 1380–1386.
(36) Salmona, M.; Malesani, P.; DeGioia, L.; Gorla, S.; Bruschi, M.; Molinari, A.; Della Vedova, F.; Pedrotti, B.; Marrari, M. A.; Awan, T.; Bugiani, O.; Forloni, G.; Tagliavini, F. *Biochem. J.* **1999**, *342*, 207–214.
(37) Florio, T.; Thellung, S.; Amico, C.; Robello, M.; Salmona, M.; Bugiani, O.; Tagliavini, F.; Forloni, G.; Schettini, G. *J. Neurosci. Res.* **1998**, *54*, 341–352.
(38) Salmona, M.; Forloni, G.; Diomede, L.; Algeri, M.; De Gioia, L.; Angeretti, N.; Giaccone, G.; Tagliavini, F.; Bugiani, O. *Neurobiol. Dis.* **1997**, *4*, 47–57.
(39) Walsh, P.; Yau, J.; Simonetti, K.; Sharpe, S. *Biochemistry* **2009**, *48*, 5779–5781.

column (Vydac). A gradient of 0 to 54% acetonitrile (ACN) with 0.1% TFA was used, and the desired product eluted at 32% ACN and was freeze-dried. The purity of PrP(106−126) peptides was confirmed by MALDI-TOF mass spectrometry.

PrP(106−126) fibrils and nonfibrillar oligomers were formed as previously described.[15,39] Briefly, for fibril preparations, HPLC-purified PrP(106−126) was dissolved in 1,1,1,3,3,3-hexafluoroispropanol (HFIP) and dried to a thin film in a conical tube. This peptide film was then suspended in 20 mM Tris buffer pH 8.0 at a concentration of 5 mg/mL. For nonfibrillar oligomer preparations, HPLC-purified PrP(106−126) was dissolved in HFIP at a concentration of 4 mg/mL, bath sonicated, and allowed to stand at room temperature for 10 min. The HFIP peptide solution was then diluted in 10 mM acetate buffer pH 4.6 at a final concentration of 1 mg/mL after the evaporation of HFIP by a gentle stream of nitrogen gas (N_2). The presence of amyloid fibrils or nonfibrillar oligomers was confirmed by transmission electron microscopy (TEM) for all samples.

Samples for solid-state NMR were lyophilized and packed into 3.2 mm rotors for analysis. Rehydrated samples were prepared by addition of an equal volume of water to dry oligomers. Membrane-disruption of rehydrated oligomers was confirmed by using a liposomal dye release assay as described previously.[39] Solution NMR samples were subjected to centrifuge spin-column (3500 Da MWCO, Amicon) to remove acetate as well as any residual monomer with the use of Milli-Q water. Samples were buffered to pH 4.6 using deuterated acetate (Cambridge Isotope Laboratories), and D_2O was added to a final concentration of 5%.

Solid-State Nuclear Magnetic Resonance (NMR). Solid-state NMR measurements were carried out on a narrow-bore Varian VNMRS spectrometer, operating at a ^{1}H frequency of 499.82 MHz. All experiments were carried out using Varian triple-resonance 3.2 mm T3MAS and BioMAS probes. Sample heating in standard T3 probes was alleviated by delivering high-flow rates of dry air at ambient temperature to the sample. All spectra were externally referenced to the downfield ^{13}C resonance of adamantine at 38.56 ppm relative to TMS.[40]

^{13}C cross-polarization was implemented using a ramped radio frequency (rf) field centered around 40−60 kHz on the low channel, matched with 50−80 kHz rf fields on the ^{1}H channel. A linear ramp on the ^{13}C channel was used in all cases, and contact times were typically 1−1.5 ms in length; $\pi/2$ pulse widths were typically 2.5−3 μs for all channels on the T3 MAS probe, or 2.5 μs (^{1}H) and 5.5 μs (^{13}C, ^{15}N) on the BioMAS probe. ^{1}H decoupling fields of 110 kHz were applied during all t_1 and t_2 periods, using a two-phase pulse modulation (TPPM) decoupling scheme.[41] In all cases, a 2-s delay was used between scans.

Two-dimensional (2D) ^{13}C−^{13}C NMR spectra were obtained using a radio frequency-assisted diffusion (RAD) recoupling sequence.[42,43] RAD mixing times of 10, 250, and 500 ms were used, at an MAS frequency of 20 kHz for nonfibrillar oligomers and 10 kHz for amyloid fibrils of PrP(106−126), with ^{1}H irradiation at a field strength matched to the spinning frequency during the RAD mixing period. Typically 200 points were obtained in the indirect dimension, with 80 scans per FID.

^{13}C T_1 relaxation times were obtained from cross-polarization spectra recorded using the spin-temperature inversion method described by Torchia,[44] with the time between the two $\pi/2$ pulses arrayed from 0 to 7.5 s. T_2 relaxation time measurements were performed using a CPMG spin−echo experiment,,[45,46] with an echo period (including π-pulse) arrayed from 50 to 5000 μs. In both T_1 and T_2 experiments, ^{1}H−^{13}C cross-polarization was achieved as described above with an MAS frequency of 10 kHz. Peak intensity was plotted as a function of the recovery time and in each case was fitted to a single exponential decay using Origin software.

Constant time ^{13}C recoupling experiments were performed using the PITHIRDS pulse sequence as described by Tycko et al.,[47] using k1 equal to 4, and k2 and k3 decremented and incremented from 23 to 0 and 0 to 23, respectively, giving 50.4 ms of total dipolar recoupling. PITHIRDS spectra were obtained at an MAS rate of 20 kHz, giving rise to 16.67 μs π pulses used during the recoupling period. Each spectrum was taken at a sweep width of 20161 Hz with 1600 points per FID. Simulations were carried out using Spinevolution as previously described.[15] Briefly, a linear string of five ^{13}C spins with variable internuclear distance was subjected to an explicit treatment of the PITHIRDS pulse sequence. In order to reduce end effects, only the dephasing of the central ^{13}C atom was observed. The resultant dephasing curves were fit to experimental data using a sum of squared residuals approach.

To directly observe solvent-accessible sites Mn^{2+}, a paramagnetic shift reagent, was added to both fibril and oligomer samples. Briefly, lyophilized fibrils and oligomers were hydrated with excess water in a 36 μL MAS rotor, with the water being added after weighing the dry sample. One dimensional (1D) ^{13}C cross-polarization spectra of the hydrated samples were recorded in the presence and absence of MnEDTA (0.2 mol per mol of peptide). A 4-s recycle delay was used in these experiments and was sufficient to prevent sample heating.

Solution NMR. Solution NMR spectra were recorded on samples containing 2.0 mM not isotope-enriched PrP(106−126) oligomers. Two-dimensional (2D) [^{1}H,^{1}H]-TOCSY with a 10 kHz DIPSI-2 mixing scheme[48] (45 ms mixing time), 2D [^{1}H,^{1}H]-NOESY[49] (600 ms mixing time), and natural abundance [^{1}H,^{13}C]-HSQC[50] spectra were recorded at 25 °C on a Varian Unity INOVA 500 MHz NMR spectrometer equipped with a room-temperature probe with *z*-axis pulsed field gradient capabilities. The H_2O resonance was suppressed by WATERGATE[51] with quadrature detection in the indirect ^{1}H dimension achieved by States-TPPI[52] in the homonuclear experiments; in the [^{1}H,^{13}C]-HSQC the H_2O resonance was suppressed by gradient coherence selection with quadrature detection in the indirect ^{13}C dimension achieved by the echo−antiecho method.[53,54]

All solution NMR spectra were processed with NMRPipe[55] software and analyzed with NMRViewJ 8.0.b16.[56] ^{1}H chemical shifts were referenced with respect to external DSS in D_2O, and ^{13}C chemical shifts were referenced indirectly.[57] Spin systems were initially identified using the ^{1}H−^{1}H TOCSY in conjunction with the ^{1}H−^{13}C HSQC. Intraresidue and sequential interresidue connectivities were then assigned using the ^{1}H−^{1}H NOESY.

The diffusion coefficient of structured PrP(106−126) monomers was measured using 1D ^{1}H pulse gradient stimulated echo

(40) Morcombe, C. R.; Zilm, K. W. *J. Magn. Reson.* **2003**, *162*, 479–486.
(41) Bennett, A. E.; Rienstra, C. M.; Auger, M.; Lakshmi, K. V.; Griffin, R. G. *J. Chem. Phys.* **1995**, *103*, 6951–6958.
(42) Takegoshi, K.; Nakamura, S.; Terao, T. *Chem. Phys. Lett.* **2001**, *344*, 631–637.
(43) Morcombe, C. R.; Gaponenko, V.; Byrd, R. A.; Zilm, K. W. *J. Am. Chem. Soc.* **2004**, *126*, 7196–7197.
(44) Torchia, D. *J. Magn. Reson.* **1978**, *30*, 613–616.
(45) Carr, H. Y.; Purcell, E. M. *Phys. Rev.* **1954**, *94*, 630–638.
(46) Meiboom, S.; Gill, D. *Rev. Sci. Instrum.* **1958**, *29*, 688–691.
(47) Tycko, R. *J. Chem. Phys.* **2007**, *126*, 064506.
(48) Rucker, S. P.; Shaka, A. J. *Mol. Phys.* **1989**, *68*, 509–517.
(49) Jeener, J.; Meier, B. H.; Bachmann, P.; Ernst, R. R. *J. Chem. Phys.* **1979**, *71*, 4546–4553.
(50) Bodenhausen, G.; Ruben, D. J. *Chem. Phys. Lett.* **1980**, *69*, 185–189.
(51) Piotto, M.; Saudek, V.; Sklenar, V. *J. Biomol. NMR* **1992**, *2*, 661–665.
(52) Marion, D.; Ikura, M.; Tschundin, R.; Bax, A. *J. Magn. Reson.* **1989**, *85*, 393–399.
(53) Kay, L. E.; Keifer, P.; Saarinen, T. *J. Am. Chem. Soc.* **1992**, *114*, 10663–10665.
(54) Schleucher, J.; Sattler, M.; Griesinger, C. *Angew. Chem., Int. Ed. Engl.* **1993**, *32*, 1489–1491.
(55) Delaglio, F.; Grzesiek, S.; Vuister, G. W.; Zhu, G.; Pfeifer, J.; Bax, A. *J. Biomol. NMR* **1995**, *6*, 277–293.
(56) Johnson, B. A.; Blevins, R. A. *J. Biomol. NMR* **1994**, *4*, 603–614.
(57) Markley, J. L.; Bax, A.; Arata, Y.; Hilbers, C. W.; Kaptein, R.; Sykes, B. D.; Wright, P. E.; Wuthrich, K. *Pure Appl. Chem.* **1998**, *70*, 117–142.

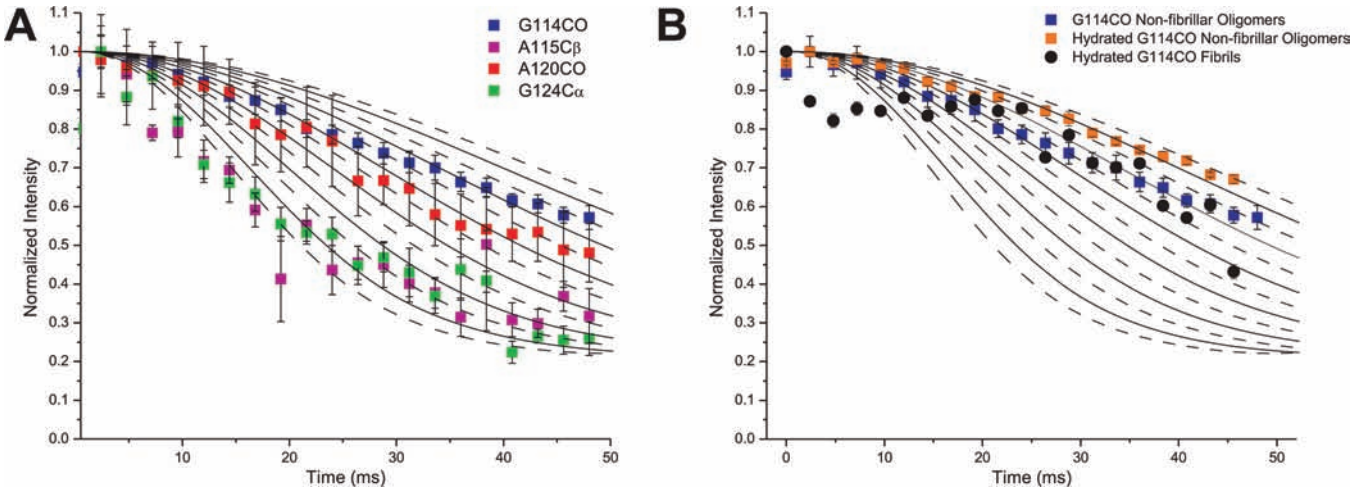

Figure 1. PITHIRDS recoupling curves for nonfibrillar PrP(106−126) oligomers. (A) ^{13}C dipolar dephasing curves obtained using PITHIRDS-CT[47] are shown for oligomers formed by PrP(106−126)^{GCO} (blue squares), PrP(106−126)^{ACO} (red squares), the A115 Cβ resonance of PrP(106−126)^{AAGG} (magenta squares), and the G124 Cα resonance of PrP(106−126)^{AAGG} (green squares). The best fits to internuclear distances simulated using Spinevolution are 7.2, 6.2, 5.6, and 5.6 Å, respectively. (B) A comparison of PITHIRDS recoupling curves for dry (blue) and hydrated (orange) PrP(106−126)^{GCO} oligomers or hydrated amyloid fibrils (black). The corresponding internuclear distances are 7.2 Å (dry oligomers), 7.6 Å (hydrated oligomers) and 7.0 Å (hydrated fibrils). Simulated data are shown in both panels as solid lines from 5.4 Å (lowest curve) to 7.8 Å (highest curve) in 0.2 Å increments. Error bars for experimental data were calculated from the rms noise in the PITHRIDS recoupling spectra. Note that in some cases, the error is smaller than the size of the symbol.

longitudinal encode−decode (PG-SLED) translational diffusion experiments[58,59] with suppression of the H_2O resonance by WATERGATE[51] at 500 MHz, 25 °C. Three nonoverlapping methyl group regions in the 1D ^1H spectra were integrated independently and the resulting intensities as a function of gradient strength fit independently by three Gaussian decays.[60] The decay constants from these fits were converted into diffusion coefficients based[60] on the absolute strength of the pulse field gradients, which had been calibrated carefully using two independent methods[58] in agreement with each other to better than 0.5%. The resulting diffusion coefficients were in turn converted into hydrodynamic radii based on the Stokes−Einstein equation, assuming a viscosity of 0.900×10^{-3} Pa s interpolated for 5% D_2O at 25 °C.[61] The diffusion coefficient and hydrodynamic radii are reported as mean ± standard error over the three nonoverlapping methyl group regions.

Results

PrP(106−126) Oligomers Contain Parallel In-Register β-Sheets. As reported previously,[39] analysis of the solid-state ^{13}C and ^{15}N chemical shifts for residues within the hydrophobic core sequence of nonfibrillar PrP(106−126) oligomers are very similar to those observed for fibrils formed by this peptide[15] and strongly suggest the presence of an extended β-strand from residues 113−125. In order to confirm that these results were not due to freeze-drying the oligomers, we have obtained chemical shift assignments for rehydrated PrP(106−126) oligomers using 1D and 2D ^{13}C MAS NMR spectra. For most sites, the ^{13}C linewidths in the dry samples are ≤2 ppm, suggesting a well-ordered and homogeneous structure. For comparison, the secondary chemical shifts for both lyophilized and rehydrated oligomers are shown in Supporting Information, Figure S1A, and confirm that the same secondary structure is present in each case. Likewise, the ^{13}C linewidths (Figure S1B [Supporting Information]) for most sites remain unchanged upon addition of excess water to the PrP(106−126) oligomers, although some broadening is observed for G119−V122 upon hydration, suggesting an increase in disorder or mobility. Residues 123−126 exhibit slightly broadened lines in both lyophilized and rehydrated oligomers, again suggestive of some conformational disorder of the peptide C-terminus in both assemblies. This is supported by a loss of signal intensity for the G126 CO−Cα crosspeak in radio frequency assisted diffusion (RAD) spectra of hydrated PrP(106−126)^{AVG2} oligomers (Supporting Information Figure S2 - likely a result of reduced dipolar couplings due to motional averaging at this site).

Based on the presence of parallel, in-register β-sheets in amyloid fibrils formed by PrP(106−126),[15] we used the PITHIRDS homonuclear recoupling scheme[47] to test for a similar arrangement in nonfibrillar oligomers. This experiment reports on the average internuclear distance between different copies of a given atom within a homo-oligomeric β-sheet. Shorter distances between labeled sites will result in an increased rate of signal dephasing due to homonuclear dipolar couplings. PITHIRDS data obtained for oligomers formed by PrP(106−126)^{GCO}, PrP(106−126)^{ACO} and PrP(106−126)^{AAGG}, are shown in Figure 1A. Fitting to the simulated dephasing curves gives distances of 5.6, 6.2 and 5.6 Å for the A115 Cβ, A120 carbonyl, and G124 Cα atoms,respectively. These distances are consistent with our previous measurements on PrP(106−126) fibrils, and indicate that the β-strands in nonfibrillar oligomers of this peptide adopt a similar in-register, parallel β-sheet structure. In particular, only this arrangement can account for the 5.6 Å distance between A115 β-carbons on adjacent strands. The best fit for the experimental G114 carbonyl data gives a distance of 7.2 Å between adjacent G114 residues, indicating an increased average interstrand distance at the

(58) Altieri, A. S.; Hinton, D. P.; Byrd, R. A. *J. Am. Chem. Soc.* **1995**, *117*, 7566–7567.
(59) Choy, W. Y.; Mulder, F. A.; Crowhurst, K. A.; Muhandiram, D. R.; Millett, I. S.; Doniach, S.; Forman-Kay, J. D.; Kay, L. E. *J. Mol. Biol.* **2002**, *316*, 101–112.
(60) Stejskal, E. O.; Tanner, J. E. *J. Chem. Phys.* **1965**, *42*, 288–292.
(61) Cho, C. H.; Urquidi, J.; Singh, S.; Robinson, G. W. *J. Phys. Chem. B* **1999**, *103*, 1991–1994.

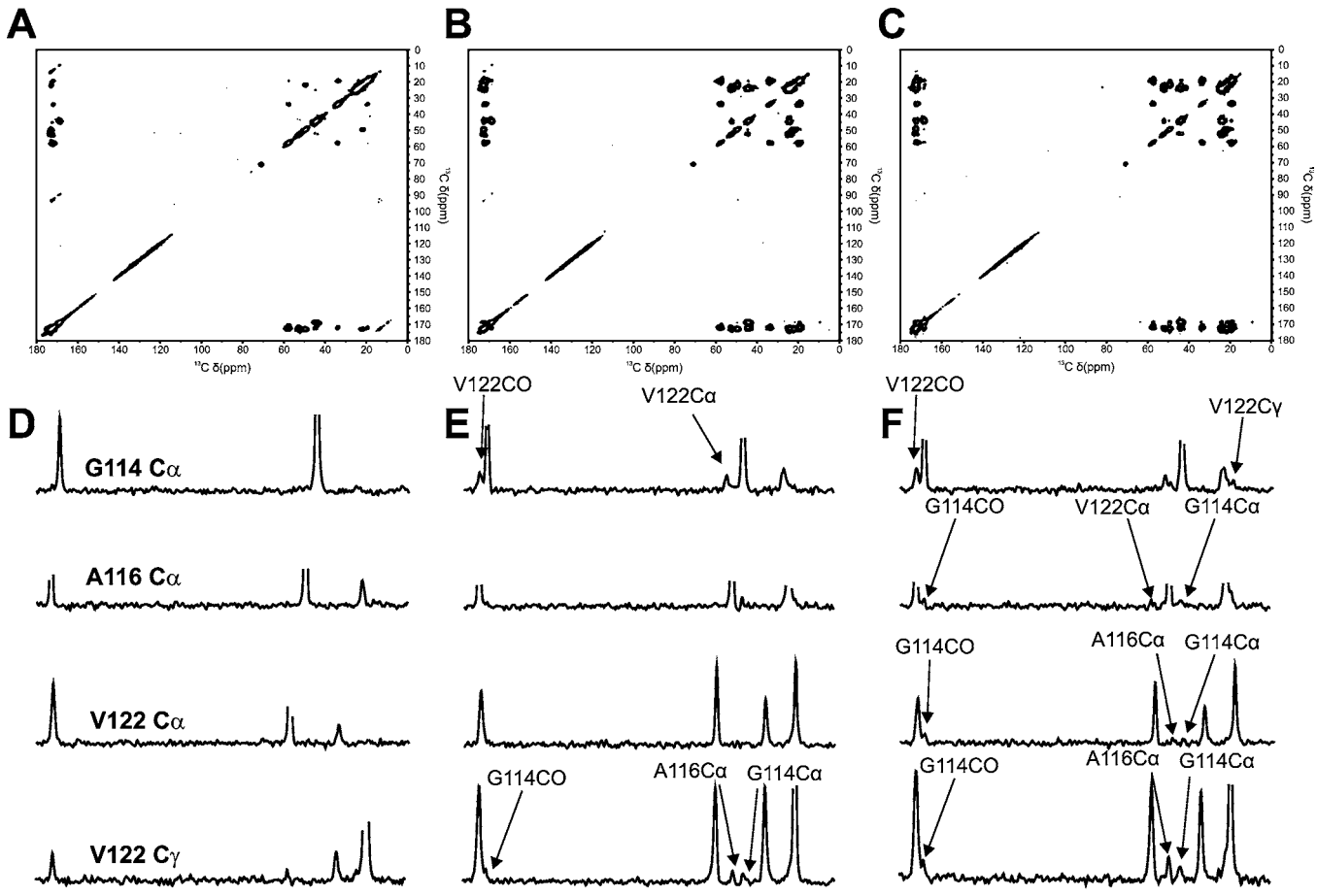

Figure 2. Long-range $^{13}C-^{13}C$ internuclear contacts observed in 2D $^{13}C-^{13}C$ NMR spectra of PrP(106−126)^{GAVL} oligomers. (A) $^{13}C-^{13}C$ correlation spectra obtained with a RAD mixing time of 10 ms. Similar spectra obtained with mixing times of 250 and 500 ms are shown in (B) and (C), respectively. Horizontal slices at the G114Cα, A116Cα, and V122Cα frequencies are shown for 10 ms (D), 250 ms (E), and 500 ms (F) mixing times. Interresidue cross peaks are indicated on the slices and discussed in the text.

N-terminus of the β-sheet, potentially a result of reduced structural order at this site.

While the data shown in Figure 1A are for lyophilized oligomers, we have also recorded PITHIRDS curves for hydrated oligomers. Sites in the core (A115, A120, G124) give similar results for both states (not shown); however, there is a slight increase in the measured G114 carbonyl distance from 7.2 Å in the dry oligomers to 7.6 Å in hydrated samples, indicating either an increased average internuclear distance upon hydration or an increase in motional averaging of the dipolar couplings in the presence of excess water (Figure 1B). In both cases, this is slightly longer than the 7.0 Å distance observed in hydrated PrP(106−126) fibrils and is suggestive of increased disorder at the N-terminus of oligomers relative to fibrillar assemblies.

PrP(106−126) Oligomers Contain Quaternary Contacts between β-Sheets That Are Similar to Those in PrP(106−126) Amyloid Fibrils. Radio frequency-assisted diffusion (RAD) spectra with various $^{13}C-^{13}C$ spin diffusion mixing times were recorded for dry and hydrated PrP(106−126) oligomers. At shorter mixing times, crosspeaks are observed between directly bonded ^{13}C atoms, permitting identification of amino acid spin systems for resonance assignments. At longer mixing times of 250−500 ms, crosspeaks are seen between all ^{13}C nuclei with internuclear distances of less than 6−7 Å. Thus these data provide valuable information regarding tertiary and quaternary structure in proteins. Figure 2 shows RAD spectra of PrP(106−126)^{GAVL} oligomers, obtained with mixing times of 10, 250, and 500 ms. At the longer mixing times, crosspeaks corresponding to long-range contacts between atoms in G114/A116 and sites within V122 are observed. Since these residues are at opposite ends of an extended parallel β-sheet, the observed connectivies must arise from intersheet contacts within the oligomer, as we have previously observed for amyloid fibrils formed by this peptide. These contacts are maintained in the presence of excess water, as shown in the 500 ms RAD spectrum of hydrated PrP(106−126)^{GAVL} oligomers (Figure 3), and provide strong evidence for an antiparallel arrangement of opposing β-sheets within the oligomeric assembly.

Identification of Structured Monomeric PrP(106−126) in Exchange with Nonfibrillar Oligomers from $^{1}H-^{1}H$ and $^{1}H-^{13}C$ Solution NMR Spectra. In order to further probe the structure and dynamics of nonfibrillar PrP(106−126), $^{1}H-^{1}H$ TOCSY, NOESY, and $^{1}H-^{13}C$ HSQC spectra were recorded for a solution of oligomers formed by unlabeled PrP(106−126). The resulting solution spectra gave surprisingly sharp, well-resolved resonances, which were unlikely to arise from the amyloid oligomers, which have an estimated molecular weight of approximately 1 MDa. To address this issue, pulse-field gradient NMR experiments were carried out, and the correlation time of the molecular species giving rise to the sharp resonances

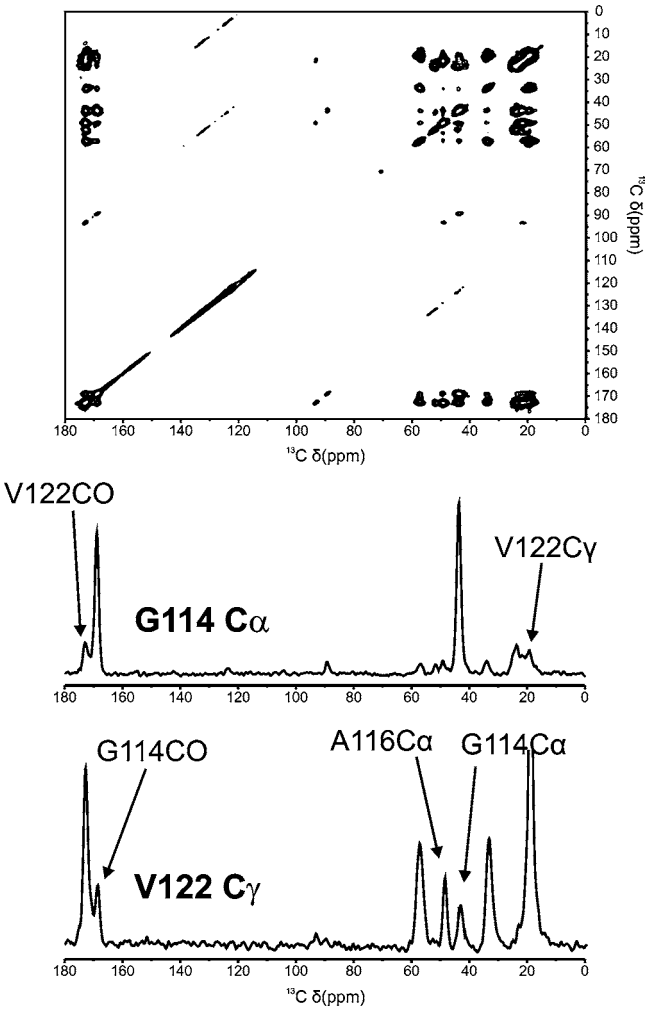

Figure 3. Long-range $^{13}C-^{13}C$ internuclear contacts are maintained in hydrated PrP(106−126)^{GAVL} oligomers. A $^{13}C-^{13}C$ correlation spectrum of hydrated PrP(106−126)^{GAVL} oligomers, obtained using a 500 ms RAD mixing time is shown in the upper panel. Horizontal slices from the G114Cα and V122Cγ frequencies are shown below. Interresidue crosspeaks are identified on the slices as in Figure 2.

was determined. The PrP(106−126) species observed by solution NMR exhibits a translational diffusion coefficient of $D = 2.15 \times 10^{-6}$ cm^2/s $\pm$ 0.11×10^{-6} cm^2/s at 25 °C (Supporting Information, Figure S3). This corresponds to a hydrodynamic radius of $R_h = 11.3$ Å $\pm$ 0.6 Å, which is identical within error to the hydrodynamic radius predicted[62] for a partially folded (11.5 Å $\pm$ 1.3 Å) or denatured (12.5 Å $\pm$ 1.1 Å) 21-residue monomer.

The aliphatic regions of the TOCSY and HSQC spectra are presented in Figure 4, and contain a number of well-resolved crosspeaks. A portion of the amide region of the HN−Hα region of the TOCSY spectrum is shown in Figure 5A. Spin systems corresponding to T107, N108, H111, and L125 were unambiguously identified using only their characteristic connectivity patterns in the TOCSY spectrum, allowing assignment of most ^{1}H and ^{13}C resonances from these residues. In addition, two inequivalent Lys and Met spin systems were identified, along with two Val, three Gly, and two Ala residues. A number of broad and poorly resolved resonances were also observed in the TOCSY spectrum, which were tentatively assigned to alanines, based on their chemical shift and spin systems.

Relatively few interresidue crosspeaks were observed in the NOESY spectrum (HN−Hα region shown in Figure 5B), suggesting a relative lack of well-ordered secondary structure in the regions of PrP(106−126) exhibiting sharp ^{1}H resonances. A small number of $H\alpha_i-HN_{i+1}$ NOEs were identified (M112/A113, A113/G114, G119/A120, A120/V121, V122/G123), allowing unambiguous assignments for K106/G114 and G119/G123, with the exception of K106 and K110, which cannot be identified with certainty. Two remaining glycines were ambiguously assigned to G120 and G126. Additional interresidue NOEs were observed between two unassigned alanine residues with very broad (TOSCY) and weak (NOESY) NMR signals. These likely represent resonances within the central A115−A118 sequence. ^{13}C resonances in the HSQC spectrum were assigned on the basis of the ^{1}H assignments where possible.

Several weak crosspeaks were also observed in the NOESY spectrum between the H111 and M109 side chains with L125 Hα/HN resonances. These connectivities are very low intensity and may result from transient intermolecular contacts between these residues during the assembly or exchange with the oligomer. It is also important to note that the Hα, Cα, and HN resonances of G114, 119, and 123 are significantly broadened in the spectra of the monomeric peptide, possibly suggesting some minor structural heterogeneity toward the core β-sheet region. This may also result from decreased mobility due to transient interactions with the larger oligomeric assembly. Some additional evidence for structural heterogeneity is seen in the presence of three distinct sets of resonances for N108, and broadening for resonances in one of the Lys spin systems. Overall, the results support the presence of a structured but somewhat disordered monomer in equilibrium with the oligomeric PrP(106−126).

All unambiguous solution and solid-state NMR ^{1}H and ^{13}C shift assignments for a solution containing PrP(106−126) oligomers are shown in Table S2 (Supporting Information). While significant deviations are observed between the ^{13}C shifts measured for several sites in the monomer relative to those obtained under MAS conditions for the oligomer, in both species the chemical shifts are largely consistent with an extended β-sheet-containing structure. Deviations in shift could stem from differences in local structure and/or from different degrees of exposure to the bulk solvent.

Despite both the relatively large changes in chemical shift at specific sites, as well as having monomers in exchange with nonfibrillar oligomers, the secondary structure appears to be relatively unaffected, based on secondary chemical shift analysis and the extended structure indicated by the presence of $H\alpha_i-HN_{i+1}$ NOEs. TALOS[63] prediction of the backbone Ψ and ϕ torsion angles for residues 107−125 was performed using solid-state ^{13}C chemical shifts for the oligomers and solution ^{1}H and ^{13}C chemical shifts for the structured monomer. In the case of ambiguous shifts (G124/126 and K106/110, and A115−118 in the monomer), calculations were performed using all permutations of these data, resulting in negligible changes in the predicted torsion angles.

(62) Wilkins, D. K.; Grimshaw, S. B.; Receveur, V.; Dobson, C. M.; Jones, J. A.; Smith, L. J. *Biochemistry* **1999**, *38*, 16424–16431.

(63) Cornilescu, G.; Delaglio, F.; Bax, A. *J. Biomol. NMR* **1999**, *13*, 289–302.

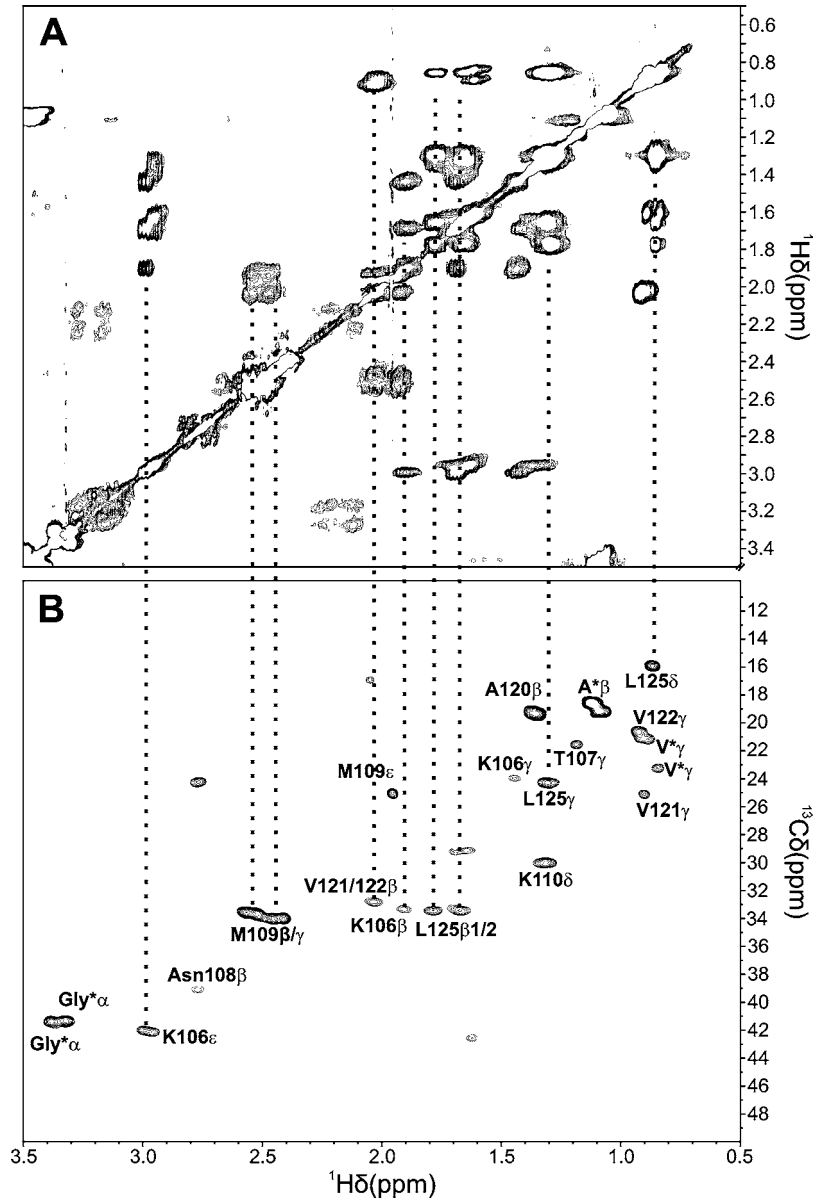

Figure 4. ^{1}H−^{1}H TOCSY and ^{1}H−^{13}C HSQC NMR spectra of PrP(106−126) monomers in equilibrium with nonfibrillar oligomers. ^{1}H and ^{13}C assignments for several sites are shown in 2D correlation spectra of PrP(106−126) oligomers in deuterated 10 mM acetate buffer (pH 4.6), recorded under solution NMR conditions. A portion of the aliphatic region of a ^{1}H−^{1}H TOCSY is shown in (A), while the corresponding region of a ^{1}H−^{13}C HSQC spectrum is shown in (B). Identified ^{1}H−^{13}C correlations are labeled in (B), with ambiguous assignments, for which only the amino acid type is known, indicated by asterisks. Connections to the corresponding spin systems in the ^{1}H−^{1}H TOCSY spectrum are indicated by dashed lines. Specific assignments were made as described in the text.

The predicted backbone torsion angles for the nonfibrillar oligomers are shown in Figure 6, along with the results for the monomeric PrP(106−126) and the previously reported ϕ and Ψ values for amyloid fibrils of PrP(106−126).[15] In each case, the results are consistent with a primarily β-strand secondary structure for all residues, with the possible exception of a turn at H111/M112 in the monomeric peptide. TALOS predicts two distinct possibilities at these sites resulting in either an extended or bent structure. The absence of supporting NOEs, as well as the likely mobility at the N-terminus of PrP(106−126), suggests that the TALOS prediction for these residues may not be entirely accurate. However, the diffusion measurements described above are more consistent with a somewhat compact form of the peptide, so the corresponding TALOS results are reported here. The chemical shift data sets for the fibrillar and oligomeric forms of this peptide do not include K106/M112, preventing a direct comparison of the N-terminal structure in these morphologies.

MAS NMR Paramagnetic Relaxation Enhancement (PRE) of PrP(106−126) Fibrils and Oligomers. PRE by Mn^{2+} was used to probe solvent exposure in MAS NMR spectra of selectively labeled PrP(106−126) fibrils and nonfibrillar oligomers. This technique has been used as a means to probe intermolecular distances in solution,[64] and in solid-state NMR as a method to probe the depth of protein insertion into model bilayer membranes.[65] Since various sites within PrP have been proposed to chelate divalent metal ions, we used MnEDTA to reduce the

(64) Iwahara, J.; Clore, G. M. *Nature* **2006**, *440*, 1227–1230.

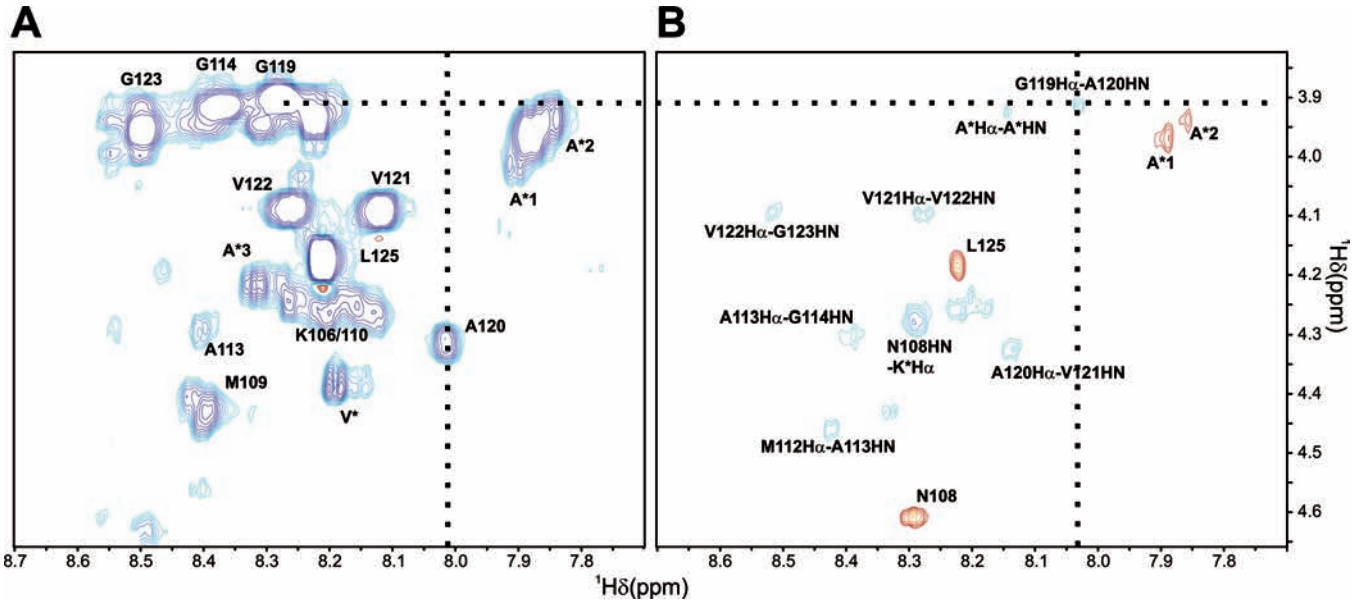

Figure 5. Sequential and intermolecular NOEs observed in a solution containing nonfibrillar oligomers of PrP(106−126). The HN-Hα region of a $^{1}H-^{1}H$ TOCSY spectrum of PrP(106−126) oligomers is shown in (A), with backbone assignments indicated. As in Figure 4, ambiguous peak assignments are indicated by asterisks, and are labeled by the amino acid spin system identified. The same expansion of a $^{1}H-^{1}H$ NOESY spectrum is shown in (B), with intra- and interresidue peak assignments as indicated. A sample interresidue NOE cross peak is indicated by the dashed lines connecting the Hα resonance of G119 with the amide of A120. Negative cross peaks are shown in red in the NOESY spectrum.

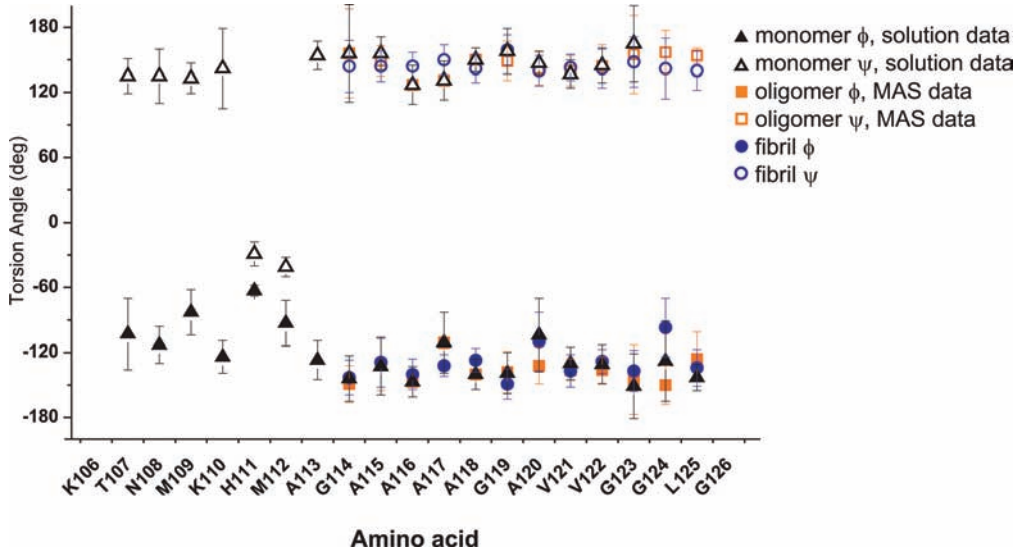

Figure 6. ϕ and Ψ backbone torsion angles predicted for PrP(106−126) oligomers and structured monomers. Angles are shown for TALOS calculations performed using only ^{13}C and ^{15}N chemical shifts obtained from MAS NMR (G114/L125 only) and for calculations performed using only the ^{1}H and ^{13}C shifts from solution NMR. For monomer sites with only ambiguous solution assignments the calculation was repeated with all possible combinations of assigned shifts, with no significant change in the resulting torsion angles. Therefore a representative set of angles is presented here. For comparison, the torsion angles previously reported for the fibrillar form of this peptide[15] are also given for residues 114−125.

likelihood of direct protein-metal interactions. One-dimensional ^{13}C spectra are shown in Figure 7 for PrP(106−126)^{AVG2} fibrils and oligomers, in the presence and absence of MnEDTA (for clarity only the aliphatic region is shown). Even at relatively low concentrations of MnEDTA (1:5 relative to protein concentration), the fibrils show ∼90% loss of signal intensity for the C-terminal G126 CO and Cα resonances, and a 20−25% reduction in signal from the V121 methyls. The latter residue is located on the outer surface of PrP(106−126) fibrils, although we cannot exclude the possibility that a significant portion of the fibril surface is occluded due to lateral association of fibrils, as seen at high concentrations by TEM. At higher concentrations of MnEDTA (not shown), there is an overall loss of signal at all sites. The PRE experiment was repeated for PrP(106−126)^{AVG} fibrils, with only V121 showing significant signal reduction.

PRE experiments were also performed on nonfibrillar oligomers formed from PrP(106−126)^{AVG} and PrP(106−126)^{AVG2},

(65) Su, Y.; Mani, R.; Hong, M. *J. Am. Chem. Soc.* **2008**, *130*, 8856–8864.

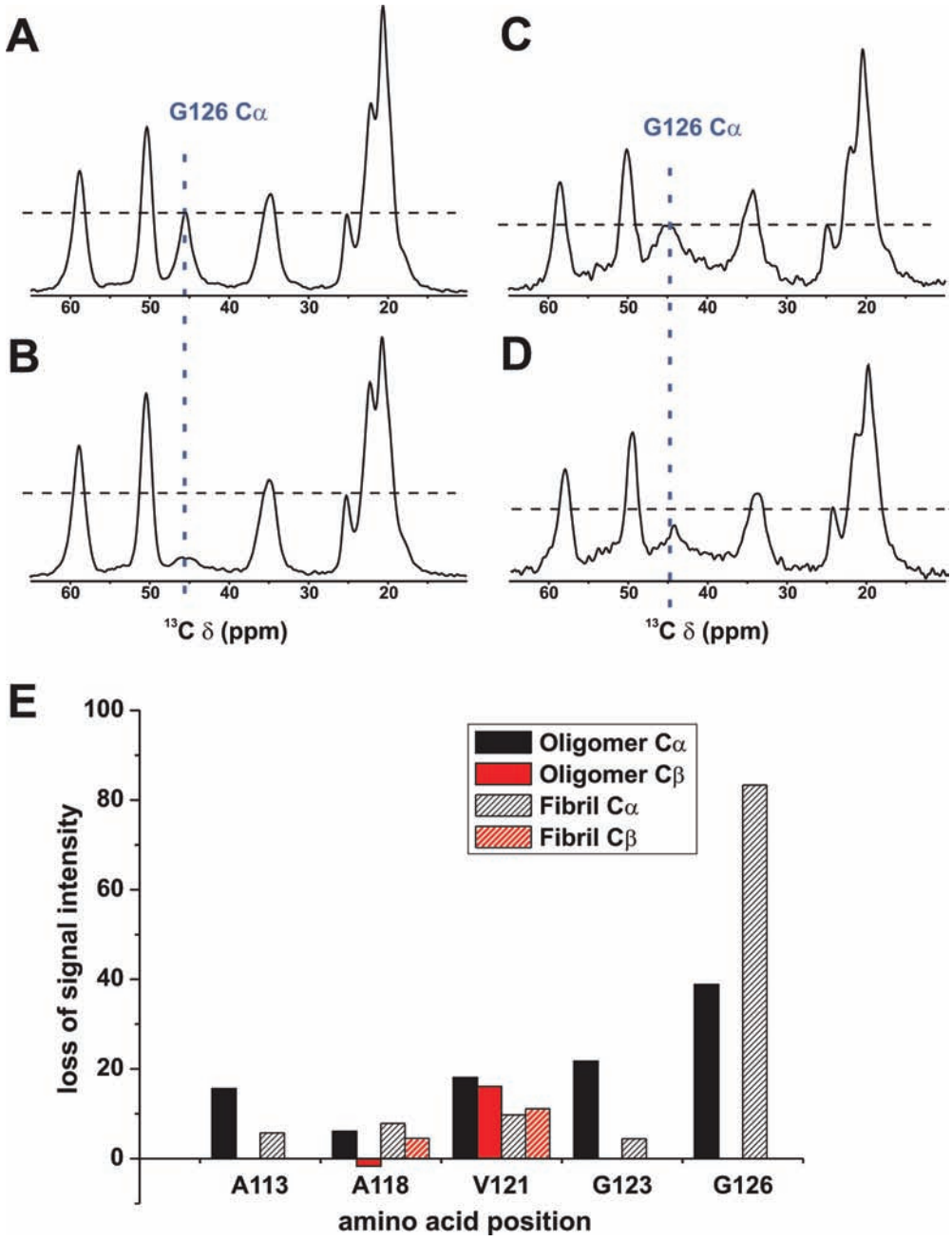

Figure 7. Mn^{2+} paramagnetic relaxation enhancement effects in ^{13}C cross-polarization (cp) spectra of $PrP(106-126)^{AVG2}$ fibrils and oligomers. ^{13}C cp spectra obtained at 10 kHz MAS for hydrated $PrP(106-126)^{AVG2}$ fibrils (A, B) and nonfibrillar oligomers (C, D). Spectra for fibrils in buffer containing MnEDTA (B) show a marked decrease in peak intensity for the G126Cα resonance relative to samples lacking MnEDTA (A). Similar spectra obtained from nonfibrillar oligomers are shown for samples with (D) and without (C) MnEDTA. In all cases, a 5:1 ratio of peptide/MnEDTA was used. The G126Cα peaks are indicated by vertical lines, and a horizontal line is set to the amplitude of this peak in the Mn^{2+} free spectrum of each pair. Quantitative analysis (E) showing signal loss for all probed sites.

using the same experimental conditions. A 40−45% loss of signal is observed for the G126 ^{13}C resonances in the nonfibrillar oligomers, with smaller (10−20%) changes in intensity at all other sites probed. This suggests that, while the loss of signal intensity at most sites was slightly larger than for the fibrils, most of the β-sheet core is somewhat shielded from the MnEDTA. The signal loss at G126 is suggestive of a peptide arrangement in which approximately half of the C-termini are exposed to the bulk solvent.

Proposed Structural Model for Nonfibrillar Oligomers of PrP(106−126). Using the torsion angles predicted by TALOS for residues 107−125, based on the combined MAS and solution NMR data sets, a set of peptide chains was constructed using CHIMERA and was energy minimized. Due to the high degree of similarity between the monomer and oligomer secondary structures, both data sets were combined to produce a single set of structural models. Single chains with representative structures including either extended or kinked torsion angles at H111/M112 are shown in Figure 8A, and are otherwise in a predominantly β-sheet conformation. Using the intermolecular distances measured from the PITHIRDS and RAD dipolar recoupling data, a tetrameric assembly containing two parallel β-sheets arranged with antiparallel face-to-face packing between the sheets was created (Figure 8B). The NOE and RAD

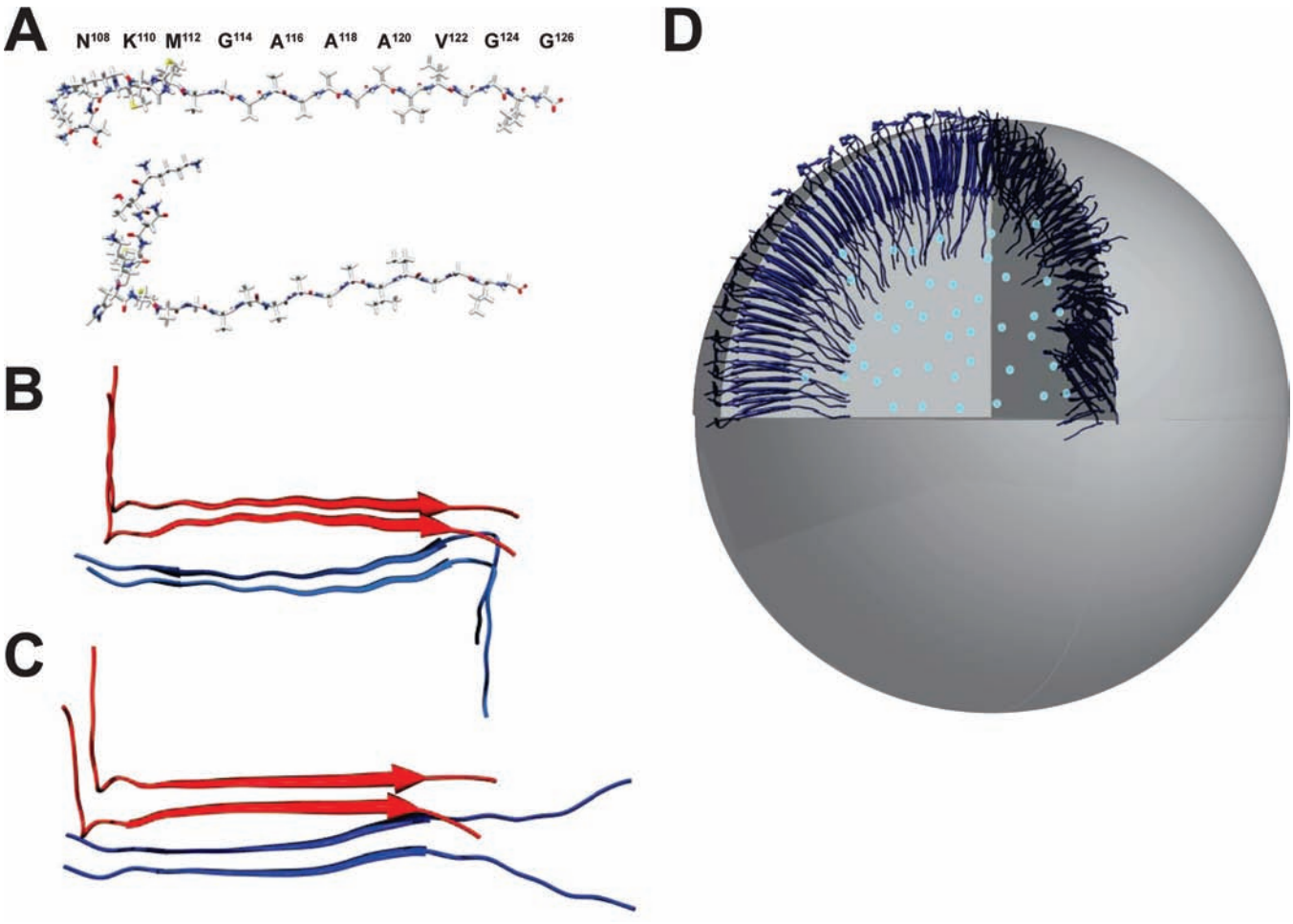

Figure 8. Structural models for nonfibrillar oligomers formed by PrP(106−126). (A) Example structural models for an individual peptide chains, based on backbone torsion angle predictions for the structured PrP(106−126) monomer. Several residues are labeled on the extended monomer structure. (B) An energy-minimized model for a fibril-like subunit consistent with the intermolecular contacts obtained from analysis of dipolar recoupling experiments. A similar model in which the N-terminal segments from one parallel pair of strands are extended is also shown in (C). (D) A schematic of a putative spherical assembly of fibril-like subunits, in which a hollow shell of radially aligned peptide chains form a micelle-like structure. Blue dots indicate the presence of water in the center of the sphere.

constraints defining the extended β-strands in the monomers and the antiparallel arrangement of sheets in the oligomers are summarized in Figure S4 (Supporting Information). Since we cannot exclude the possibility of poor TALOS predictions for H111 and M112 torsion angles, an alternate arrangement with one pair of strands containing an extended N-terminus is shown in Figure 8C. A tetramer was used in each case as the minimum assembly that can satisfy the dipolar recoupling data, although the presence of more extended fibril-like structures cannot be excluded.

Our previous TEM, DLS, and AFM measurements indicate that the oligomers are spherical objects at least 20−30 nm diameter.[39] The NMR data presented here indicate a predominantly extended peptide structure with a local interchain packing reminiscent of amyloid fibrils with approximately 50% surface exposure of the C-termini. Additionally, the relatively narrow linewidths observed for both ^{13}C under MAS, and for ^{1}H and ^{13}C under solution NMR conditions are suggestive of single conformations/environments for residues in the core, with the potential for some heterogeneity and mobility at the N- and C-termini. The model that best fits all of these requirements is a variation on the micelle-like arrangement of peptide chains previously proposed for spherical oligomers of Aβ.[31,66] Such an arrangement is depicted in Figure 8D, in which the tetramers from 8C are aligned radially within a hollow, water-filled sphere with a diameter consistent with DLS and TEM measurements.

Discussion

While the formation of nonfibrillar oligomers has been proposed as a common element of the aggregation pathway of amyloid peptides, and an important element of amyloid cytotoxicity, few structural details of these assemblies have been reported. Recently, we have described optimized solution conditions for forming stable oligomers of PrP(106−126) in preparations that are free from fibrils, and which are therefore suitable for structural studies.[39] Under these conditions, similar to those used by Kayed et al. for cytotoxicity studies, spherical oligomers are formed with an apparent hydrodynamic radius of approximately 30 nm. Preliminary solid-state NMR and CD measurements indicated a predominantly β-sheet secondary structure. Consistent with previous reports of membrane disruption and cytotoxicity of nonfibrillar amyloid oligomers,[1,8,31]

(66) Laurents, D. V.; Gorman, P. M.; Guo, M.; Rico, M.; Chakrabartty, A.; Bruix, M. *J. Biol. Chem.* **2005**, *280*, 3675–3685.

PrP(106−126) oligomers exhibited a potent ability to cause liposome leakage, while monomers and fibrils formed by this peptide are relatively inert. Thus, we expect that these represent the cytotoxic form of PrP(106−126).

Our present results provide local structural constraints which define the presence of parallel in-register β-sheets, packed in an antiparallel arrangement. This arrangement of chains is present in both lyophilized and rehydrated PrP(106−126) oligomers and is essentially indistinguishable in our experiments from the interchain packing previously observed for amyloid fibrils of this peptide.[15] We propose, on the basis of NMR and biophysical data, that a hollow, water-filled micelle-like assembly is the most likely internal structure for the large spherical oligomers of PrP(106−126). A similar micellar arrangement of fibril-like subunits has recently been proposed for large oligomers formed by Aβ,[31] on the basis of the presence of parallel in-register β-strands in lyophilized oligomers formed by that protein. One distinct difference between the oligomers formed by these two different peptides, however, is the lack of thioflavin T (ThT) binding to PrP(106−126) oligomers, while the nonfibrillar oligomers of Aβ bind ThT. This suggests either differing amounts of cross-β structure, or poor accessibility to dye in the case of PrP(106−126). For instance, in a micelle-like structure, the more ordered β-sheet core may be shielded from large solutes by the disordered N-termini on the surface of the sphere.

It is important to note that, while the overall similarity of our proposed model for PrP(106−126) oligomers and previous models of Aβ may argue in favor of a common structure for nonfibrillar amyloid oligomers, it is likely that many local conformations and quaternary structures are accessible to amyloid proteins during the misfolding process. This is clearly illustrated when our results and those of Chimon et al.[31] are compared to recent solution NMR studies of the local structure of small (16−64 kDa) Aβ(1−42) oligomers.[32] In that study, SDS-stabilized small oligomers were shown to form extended β-strands, but to have a combination of fibril-like and nonfibrillar contacts between strands. Likewise, recent solid-state NMR data reported for nonfibrillar oligomers of α-synuclein, seem to indicate a significantly different secondary structure for oligomers relative to fibrillar protein, and may support significantly decreased order in the oligomers.[33] Additionally, some amyloidogenic sequences are able to induce membrane fusion or induce negative curvature upon binding to membranes in apparently monomeric disordered or helical conformations, based on solution NMR studies of their structure when associated with micelles.[67−69] Taken together, this suggests that there may be several distinct modes of amyloid activity at membranes.

Despite the relatively small changes in secondary and quaternary structure for PrP(106−126) oligomers relative to amyloid fibrils, we do see strong indications of decreased order and increased local mobility or conformational heterogeneity in the oligomers. This is highly dependent on the hydration state of the sample, which contrasts with the relative insensitivity of most amyloid fibrils to the presence of bulk water.[15,70,71] Upon complete hydration of the oligomers with an equal mass of water, but in the absence of bulk water, we observed relatively small local changes in secondary and quaternary structure for residues 113−126 using MAS NMR experiments, and only small increases in the ^{13}C linewidths for sites within the hydrophobic core of the peptide. This is supported by relatively small changes in the ^{13}C T_1 and T_2 NMR relaxation times (Figure S5, Supporting Information).

In the presence of bulk water, our solution NMR experiments indicate the presence of a small population of partially structured monomers in exchange with the large spherical oligomers, as supported by NMR diffusion measurements. No other set of resonances is observed in the solution spectra, demonstrating the absence of any significant amount of unstructured monomer in the oligomer preparations. The presence of an equilibrium between the monomer and oligomer states is supported by the fact that extensive dialysis does not change the intensity of the NMR signals from the monomer. Despite containing significant secondary structure, the absence of long-range NOEs, the presence of significant line broadening at several sites and the identification of multiple resonances for other residues, suggests that the monomeric peptide remains poorly ordered and likely samples multiple conformations when released from oligomers. The appearance of intraresidue NOE signals with negative intensity also supports the presence of rapid local motions in the monomeric peptide, providing further evidence of a partially structured but poorly ordered entity. The broad resonances observed within the GAAAAG palindromic sequence may alternately suggest that this is an important site of interaction with the larger assembly, with line broadening resulting from transient associations.

In terms of the biological activity of PrP(106−126) assemblies, the model proposed in Figure 8D suggests some potential mechanisms for the membrane disruption cytotoxicity attributed to large nonfibrillar oligomers. It is known that hydrophobic interfaces and surfaces can catalyze fibril formation, or that they may increase the rate of fibril growth, possibly through increased local concentration and organization of monomers in a two-dimensional environment. Under these conditions, the dissociation of oligomers into small 'seeds' that can subsequently nucleate fibril formation at a membrane surface might readily occur, creating a loss of bilayer integrity and resulting in cell death. This possibility is supported by previous reports that Aβ fibrillization can cause defects in supported planar bilayers.[26] An alternate hypothesis is that, upon association of oligomers with membranes, short fibril-like segments are able to insert into the bilayer, forming a barrel-stave or toroidal pore. Pore formation by amyloid peptides has been suggested as a likely mechanism or membrane disruption and cell death by amyloid peptides, based on reports of single-channel conductance induced by amyloid peptides and by a number of molecular modeling studies.[8,72] On the basis of recent reports that fragmented amyloid fibrils exhibit significantly increased cytotoxicity relative to intact fibrils,[73] it is likely that the large nonfibrillar oligomers act as reservoirs of small fibril-

(67) Nanga, R. P.; Brender, J. R.; Vivekanandan, S.; Popovych, N.; Ramamoorthy, A. *J. Am. Chem. Soc.* **2009**, *131*, 17972–17979.
(68) Brender, J. R.; Lee, E. L.; Cavitt, M. A.; Gafni, A.; Steel, D. G.; Ramamoorthy, A. *J. Am. Chem. Soc.* **2008**, *130*, 6424–6429.
(69) Brender, J. R.; Hartman, K.; Gottler, L. M.; Cavitt, M. E.; Youngstrom, D. W.; Ramamoorthy, A. *Biophys. J.* **2009**, *97*, 2474–2483.
(70) Petkova, A. T.; Yau, W. M.; Tycko, R. *Biochemistry* **2006**, *45*, 498–512.
(71) Paravastu, A. K.; Petkova, A. T.; Tycko, R. *Biophys. J.* **2006**, *90*, 4618–4629.
(72) Jang, H.; Zheng, J.; Lal, R.; Nussinov, R. *TIBS* **2008**, *33*, 91–100.
(73) Xue, W. F.; Hellewell, A. L.; Gosal, W. S.; Homans, S. W.; Hewitt, E. W.; Radford, S. E. *J. Biol. Chem.* **2009**, *284*, 34272–34282.

like segments capable of exerting a similar effect on cell membranes. Such a possibility may in part explain the common action observed for large oligomers formed by several different amyloid peptides.[1]

Due to the importance of nonfibrillar oligomers in the pathogenesis of amyloid diseases, it is essential to develop a detailed understanding of their relationship to the amyloid fibrils that are the hallmark of these diseases. While there has been evidence presented suggesting that soluble oligomers may represent misfolding intermediates on the pathway to fibril formation,[74,75] other studies suggest that they form via an off-pathway misfolding event.[76,77] The presence of fibril-like structures in nonfibrillar oligomers of PrP(106−126), as well as in large oligomers of Aβ, seems to suggest that structural rearrangement of oligomers into mature amyloid fibrils may be possible in these systems, although the inherent stability of the nonfibrillar PrP(106−126) assemblies implies a barrier to this change in assembly. Thus, while it is clear that these two different oligomeric states are surprisingly similar in local structure, the relationship between them remains to be determined. Using well-defined systems such as PrP(106−126), in which stable fibrils and oligomers can be prepared under varying solution conditions, detailed examination of amyloid misfolding pathways should be possible.

(74) Frare, E.; Mossuto, M. F.; de Laureto, P. P.; Tolin, S.; Menzer, L.; Dumoulin, M.; Dobson, C. M.; Fontana, A. *J. Mol. Biol.* **2009**, *387*, 17–27.
(75) Auer, S.; Meersman, F.; Dobson, C. M.; Vendruscolo, M. *PLoS Comput. Biol.* **2008**, *4*, e1000222.
(76) Necula, M.; Kayed, R.; Milton, S.; Glabe, C. G. *J. Biol. Chem.* **2007**, *282*, 10311–10324.
(77) Glabe, C. G. *J. Biol. Chem.* **2008**, *283*, 29639–29643.

Conclusions

We report here a comprehensive solution and solid-state NMR investigation supporting the presence of local fibril-like secondary and quaternary structure in large nonfibrillar oligomers formed by the amyloid peptide PrP(106−126). On the basis of these results combined with PRE data, the effects of hydration on local dynamics, and previous biophysical characterization of these oligomers, we propose a micelle-like assembly composed of radially aligned fibril-like subunits in rapid equilibrium with a small population of monomers with similar secondary structure. Our model is consistent with a hydrated, partially disordered spherical assembly and is similar to structures proposed for large oligomers of Aβ in the past, potentially pointing to a common structural motif for neurotoxic amyloid oligomers. This suggests that the presence of nascent fibril-like structures within a nonfibrillar assembly may play an important role in membrane disruption and cytotoxicity of PrP(106−126) and other amyloid peptides.

Acknowledgment. This work was supported by operating grants from the Natural Sciences and Engineering Research Council of Canada and PrioNet Canada. The authors thank Dr. Ranjith Muhandirim for assistance with acquisition of solution NMR spectra. P. Walsh is funded by the Restracomp program at the Hospital for Sick Children. S. Sharpe is a Canada Research Chairs Program chair holder.

Supporting Information Available: Supplementary Figures S1−S5, Tables S1 and S2, and complete ref 32. This material is available free of charge via the Internet at http://pubs.acs.org.

JA100431Q